

Molecular Beam Photochemistry of Organopolysilanes and Organopolygermanes

Ian Borthwick, Lawrence C. Baldwin, Mark Sulkes,* and Mark J. Fink*

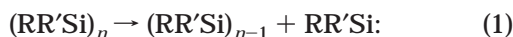
Department of Chemistry, Tulane University, New Orleans, Louisiana 70118

Received November 2, 1999

The molecular beam photochemistry of various polysilanes and polygermanes was investigated. In most cases, the precursor compounds were photolyzed in the nozzle region of a supersonic jet by a 193 nm laser and the photoproducts analyzed downstream by 118 nm photoionization pulses followed by time-of-flight mass spectrometry. The polysilane and polygermane compounds included in this study were $\text{PhMeSi}(\text{SiMe}_3)_2$, $\text{PhSi}(\text{SiMe}_3)_3$, $(\text{Me}_2\text{-Si})_6$, $(\text{Me}_2\text{Ge})_6$, and 1,3-diphenyl-1,2,2,3-tetramethyl-1,2,3-trisilacycloheptane. The 193 nm photoproducts of PhSiMe_3 , $\text{Me}_3\text{SiSiMe}_3$, and vinyltrimethylsilane were also examined for comparison purposes. Dimethylsilylene ($\text{Me}_2\text{Si:}$) was directly observed as the major one-photon photoproduct from the cyclic precursors $(\text{Me}_2\text{Si})_6$ and 1,3-diphenyl-1,2,2,3-tetramethyl-1,2,3-trisilacycloheptane. Likewise, dimethylgermylene ($\text{Me}_2\text{Ge:}$) was directly observed in the photolysis of $(\text{Me}_2\text{Ge})_6$. One-photon photolysis of the noncyclic polysilanes $\text{PhMeSi}(\text{SiMe}_3)_2$ and $\text{PhSi}(\text{SiMe}_3)_3$, however, gave radical products derived from the homolytic scission of a single Si–Si bond with little or no evidence of silylene being generated directly. A mechanism explaining the difference in photochemical outcome for cyclic vs noncyclic molecules is presented. Finally, molecular Si_2C is found to be a ubiquitous product resulting from the multiphoton photochemistry of a number of organosilicon precursors.

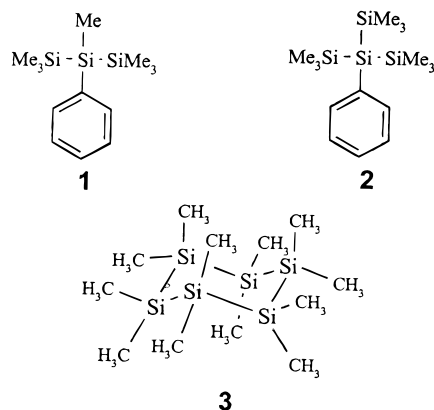
Introduction

Organosilylenes, $\text{R}_2\text{Si:}$, are divalent reactive intermediates which have been implicated in such diverse processes as the direct synthesis reaction,¹ the CVD of thin films from organosilanes,² and the photochemical degradation of polysilanes.³ Organosilylenes have been previously generated both in solution⁴ and in cold inert matrixes⁵ by photolysis of either cyclopolysilanes (eq 1) or 2-aryltrisilanes (eq 2).



Extension of these photochemical reactions to the gas phase would allow the generation of a variety of organosilylene species for molecular beam study. Mass-selected molecular beam experiments could then be carried out to assess/identify reaction products of silylenes with selected coreactants added to the beam. Alternatively, molecular beam laser spectroscopy could be carried out on cold, collisionless silylene species (e.g. ionization potentials, vibrationally resolved excitation spectra). In a preliminary study, we examined the gas-phase photolysis of the following known condensed-

phase precursors to silylenes in a molecular beam: $\text{PhMeSi}(\text{SiMe}_3)_2$ (**1**), $\text{PhSi}(\text{SiMe}_3)_3$ (**2**), and $(\text{Me}_2\text{Si})_6$ (**3**).⁶



The photochemical generation of $\text{Me}_2\text{Si:}$ from $(\text{Me}_2\text{Si})_6$ was inferred indirectly through the mass spectrometric detection of the ring-contracted $(\text{Me}_2\text{Si})_5$ fragment. In stark contrast, the linear trisilane **1** and the branched tetrasilane **2** only gave silyl radical products resulting from the homolytic cleavage of a single Si–Si bond. No silylene products were detected even at the highest laser fluences utilized.

We have now carried out additional experiments which are more general in two respects. First, the previous experiments employed the same 266 nm pulses (Nd:YAG fourth harmonic, 4.66 eV per photon) downstream across the molecular beam both to photolyze the

(1) Bazant, V.; Joklik, J.; Rathousky, J. *Angew. Chem., Int. Ed. Engl.* **1968**, 7, 112.

(2) Scott, B. A.; Pecelik, R. M.; Simonyi, E. E. *Appl. Phys. Lett.* **1981**, 39, 73 and references therein.

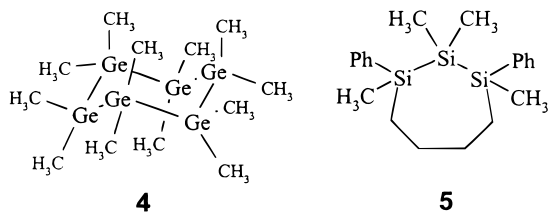
(3) Miller, R. D.; Michl, J. *Chem. Rev.* **1989**, 89, 1359.

(4) Gaspar, P. P.; Holten, D.; Konieczny; Corey, J. Y. *Acc. Chem. Res.* **1987**, 20, 329.

(5) Michalczyk, M. J.; Fink, M. J.; DeYoung, D. J.; Welsh, K.; West, R.; Michl, J. *Silicon, Germanium, Tin Lead Compd.* **1986**, 9, 75.

(6) Huang, Y.; Sulkes, M.; Fink, M. J. *J. Organomet. Chem.* **1995**, 499, 1.

precursors as well as to photoionize species present for mass analysis. The new experiments were two laser experiments. The photolysis pulses were now directed just below the gas expansion nozzle, prior to gas skimming to form a molecular beam. The analyzing photoionization was carried out with 118 nm pulses which were directed further downstream across the molecular beam, adjacent to the draw-out electrode. The 118 nm pulses have a one-photon energy of 10.5 eV, sufficient to photoionize almost any species that might be present without significant fragmentation, leading to their time-of-flight mass detection. Second, a wider range of precursors has been studied. In addition to compounds **1–3**, we have also examined the additional ring compounds (Me₂Ge)₆ (**4**) and 1,2,2,3-tetramethyl-1,3-diphenyl-1,2,3-trisilacycloheptane (**5**) as well as



some mono- and disilanes, which help to qualify product analyses in the other cases. Using beam techniques, we have been able to study the photolysis mechanism independent of the ionization process and have demonstrated unambiguous detection of dimethylsilylene and dimethylgermylene.

Experimental Section

Synthesis. All manipulations were conducted under an inert atmosphere of argon employing standard Schlenk techniques. All glassware was oven-dried at 140 °C prior to use. Tetrahydrofuran was distilled from sodium benzophenone ketyl under nitrogen. Pentane was distilled from CaH₂ under nitrogen. Methylene chloride was washed with concentrated H₂SO₄, H₂O, and aqueous K₂CO₃(aq), dried over CaCl₂, and finally distilled over P₂O₅ under argon. ¹H, ¹³C, and ²⁹Si NMR data were recorded on a GE Omega 400 NMR spectrometer. GCMS data were obtained using an HP5890 Series 2 GC/HP5989A mass spectrometer with an ULTRA 2 cross-linked 5% PhMe siloxane column. Silica gel (40 μm, 230–400 mesh) was purchased from Scientific Adsorbents Inc. The polysilanes **1** and **2** were synthesized according to previously reported procedures.⁷ Dodecamethylcyclotrihexasilane (**3**) was purchased from Petrarch, now United Chemical Technology, Inc. Dodecamethylhexagermane, vinyltrimethylsilane, phenyltrimethylsilane, and hexamethyldisilane were obtained from Aldrich and used without further purification. The synthesis of 1,3-diphenyl-1,2,2,3-tetramethyltrisilacycloheptane (**5**) was accomplished using a modified literature procedure.⁸

(Ph₂MeSi)₂SiMe₂. Ph₂MeSiCl (0.076 mol, 16.0 mL) was added dropwise with stirring for 15 min to a suspension of cut lithium wire (0.43 mol, 3.0 g) and 20 mL of THF in a 250 mL three-neck round-bottom flask. After 18 h of stirring at room temperature, an additional 60 mL of dry THF was added. The resultant dark brown-green solution was cannulated into an addition funnel and added dropwise with stirring for 1 h to a flask containing Me₂SiCl₂ (0.041 mol, 5.0 mL). The solution

was stirred for an additional 21 h and the THF removed by rotary evaporation. The resulting solid was quenched with H₂O and extracted with cyclohexane. The tannish organic layer was dried over MgSO₄ and the solvent removed. Crystallization from EtOH yielded 4.75 g (28%) of the white solid. Mp: 62.4–62.8 °C. GCMS: *m/z* 452 (M⁺). ¹H NMR (δ (ppm), d₆-acetone): 7.35 (m, 10H), 0.44 (s, 6H), 0.25 (s, 6H). ¹³C NMR (δ (ppm), d₆-acetone): 137.1 (Ph), 134.9 (Ph), 128.8 (Ph), 127.3 (Ph), –4.1 (SiMe), –4.9 (SiMe₂). ²⁹Si NMR (δ (ppm), CDCl₃): –24.3 (SiMe), –60.7 (SiMe₂).

1,4-Bis(bromomagnesio)butane. A solution of 1,4-dibromobutane (0.011 mol, 1.3 mL) in 8 mL of THF was added dropwise to a suspension of 0.029 mol (0.70 g) of Mg turnings in 50 mL of THF for 30 min at room temperature. The solution was stirred for 48 h.

1,3-Diphenyl-1,3-bis(triflate)tetramethyltrisilane. (Ph₂MeSi)₂SiMe₂ (0.011 mol, 5.0 g) and 65 mL of freshly distilled CH₂Cl₂ were placed in a 250 mL three-necked flask equipped with an addition funnel and reflux condensor. This solution was cooled to 0 °C; then triflic acid (0.022 mol, 1.95 mL) was added dropwise over 10 min with stirring. The solution was stirred overnight at room temperature, the CH₂Cl₂ was removed under vacuum, and 70 mL of dry pentane was added. The ditriflate was used in the next step without further purification.

1,3-Diphenyl-1,2,2,3-tetramethyl-1,2,3-trisilacycloheptane. The solution of 1,4-bis(bromomagnesio)butane was cannulated into the addition funnel attached to the round-bottom flask containing the ditriflate. The di-Grignard was then added dropwise over a 1.3 h period. The resulting solution was stirred overnight at room temperature. The solvent was then removed under vacuum, and the product was quenched with H₂O and extracted with diethyl ether. The product was then purified over a silica gel column with hexane as the eluent, which yielded a 0.79 g (20%) mixture of *cis* (45%) and *trans* (55%) isomers as a clear oil. GCMS: *m/z* 354 (M⁺), both isomers. UV: λ_{max} 239. ¹H NMR (δ (ppm), CDCl₃): 1.8 (m, 8H), 1.3 (m, 4H), 1.1 (m, 4H), 0.50 (s, 3H), 0.45 (s, 6H), 0.30 (s, 3H), 0.14 (s, 6H), –0.04 (s, 3H). ¹³C NMR (δ (ppm), CDCl₃): 139.5 (Ph), 139.3 (Ph), 134.2 (Ph), 128.5 (Ph), 128.0 (Ph), 25.5 (CH₂), 12.4 (CH₂), –3.8 (SiMe), –5.3 (SiMe), –5.4 (SiMe). IR (neat, cm^{–1}): 1717 (s), 1423 (s), 1362 (s), 1222 (s), 531 (s).

Molecular Beam Studies. All experiments were performed in a molecular beam photoionization time-of-flight mass spectrometer system (R. M. Jordan and Co.). Precursor samples entrained in He gas were introduced through a pulsed solenoid gas valve (General Valve Series 9).⁹ To attain sufficient sample vapor pressure when it was not available at room temperature, the sample holder and, downstream from it, the pulsed nozzle could be heated. The photolysis laser (Lambda Physik Lextra 200) was operated with ArF to produce 193 nm photons. In a few experiments 222 nm photolysis pulses were also employed (Questek Series 2000 excimer using KrCl). Unless noted otherwise, the photolysis wavelength used was 193 nm. The 193 nm laser beam was loosely focused by a 30 cm lens just below the pulsed valve, producing a spot across the gas jet of approximately 2 mm². The power measured immediately before the lens was up to 20 mJ. The ensuing gas pulses, now containing photolysis products, were passed through a 0.5 × 4 mm slit skimmer to form a molecular beam. The downstream distance between the pulsed valve and the photoionization beam was approximately 8 cm. The delay between the photolysis and ionization lasers was varied using a Stanford DG535 delay generator; it was typically 40 μs. The 118 nm vuv photoionization pulses were produced by frequency-tripling the 355 nm output from a Continuum YG680 Nd:YAG laser (third harmonic) in a mixture of 9% Xe in Ar.¹⁰ The 355 nm pulses were focused into the tripling cell with a 15 cm lens,

(7) (a) Duffaut, N.; Donogues, J.; Calas C. *R. Acad. Sci. Paris, Ser. C* **1969**, 967. (b) Puranik, D. B.; Johnson, M. P.; Fink, M. J. *Organometallics* **1989**, 8, 770.

(8) Sakurai, H.; Kobayashi, Y.; Nakadaira, Y. *J. Am. Chem. Soc.* **1974**, 96, 2657.

(9) Huang, Y.; Sulkes, M. *Rev. Sci. Instrum.* **1994**, 65, 3868.

(10) Bramer, S. E.; Johnston, M. V. *Appl. Spectrosc.* **1992**, 46, 255.

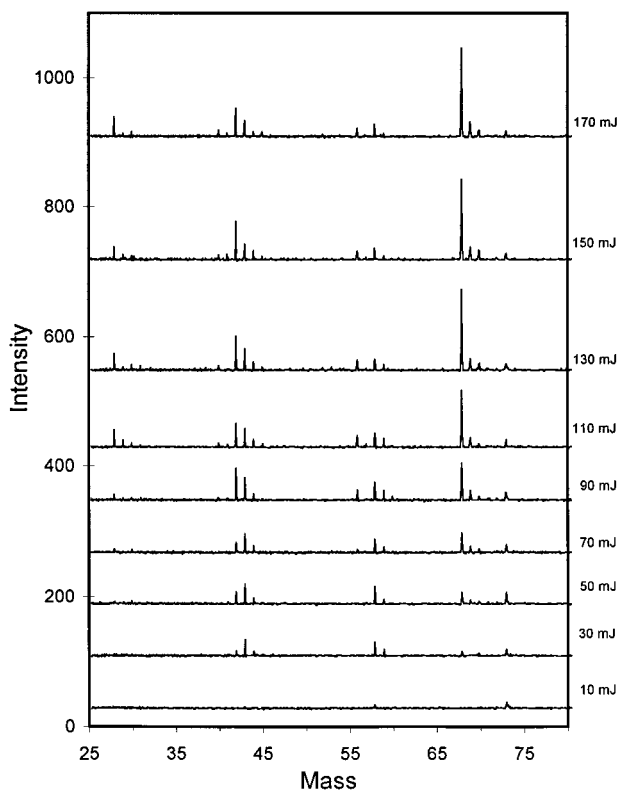


Figure 1. Mass spectra series following 193 nm photolysis of compound **3** and subsequent 118 nm photoionization. The spectra shown correspond to increasing 193 nm pulse energy (internal readings from Lextra 200 laser) from bottom to top (lowest 10 mJ), as indicated in the figure legend.

and the cell was isolated from the molecular beam chamber by a 63 mm focal length LiF lens. By offsetting the 355 nm beam from the center of the quartz lens, it was possible to have the two beams traverse slightly different paths through the mass spectrometer, so that two-color photoionization did not occur. The ions produced were mass-detected in a reflectron time-of-flight mass spectrometer; the signal from the micro-channel plate detector was digitized by a Tektronix 2440 digital oscilloscope.

Results

Photolysis of (Me₂Si)₆. Figure 1 shows mass spectra as a function of photolysis beam power. A small product peak, out of the figure range, also appears at 290 amu, corresponding to (Me₂Si)₅, but the major photolysis products all appear below 100 amu. Even with no photolysis pulse at the nozzle (lowest trace) photoproducts still appear, principally at 73 amu, corresponding to a Me₃Si radical. These photoproducts arise from the 118 nm pulse. Growth of strong peaks can be seen at 28 amu (Si), 42 amu (SiCH₂), 43 amu (MeSi), 58 amu (Me₂Si), and 68 amu (Si₂C). Peak sizes for one species compared to another do not necessarily reflect directly relative species populations.

Separate series of power dependence measurements were made for each of the foregoing mass products. Each independent series was plotted in a log(peak area) versus log(pulse energy) form. A representative plot for the 58 amu mass product is shown in Figure 2. Generally for a given mass peak multiple independent power dependence series were carried out. If a product arose

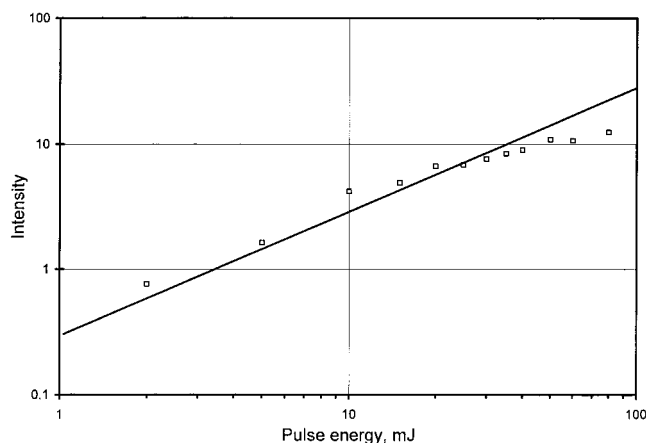


Figure 2. log(intensity) versus log(pulse energy) dependence monitoring the 58 amu product peak of (Me₂Si)₆ following 193 nm photolysis. The 193 nm pulse energies are the internal energy readings from the Lextra 200 laser. As can be seen by the reference line of slope 1.00, experimental fits are close to this slope. A slope of 1 indicates that the photolysis process was one photon.

from only a single photolysis mechanism, the slope of the plots should equal the number of photolysis photons involved. Typically for a larger peak, particularly mass 68 here, the plots are of better quality. In general, low pulse energy points may be less reliable due to smaller product peak sizes; plateau effects, due to saturation, may take place at higher pulse energies.

For the mass peak of paramount interest, mass 58 (Me₂Si), four separate series of 193 nm power dependence measurements were all consistent with a one-photon photolysis process. The 43 amu (MeSi) peak appeared concomitantly with the 58 amu (Me₂Si) peak and was prominent at low laser fluences, suggesting that this mass is a daughter ion of dimethylsilylene. The 290 amu (Me₂Si)₅ peak decreased with increasing 193 nm photolysis energy, consistent with additional photochemistry further reducing its population.

The 68 amu peak is due to Si₂C. Corroboration is found by examination of peak ratios at masses 68, 69, and 70, the latter peaks arising primarily from ²⁹Si and ³⁰Si. (At higher laser powers saturation effects can cause the relative sizes of smaller mass isotopic peaks to be unduly large.) A Si₂C species would be expected to arise from multiphoton processes; two series of power dependence measurements are closely consistent with a two-photon process. Mass peaks at 28 amu (Si), 40 amu (SiC), and 56 amu (Si₂) closely parallel the growth of the 68 amu peak and are likely daughter ions of Si₂C. The 68 amu peak is noteworthy because of its size and its appearance in the photolysis of a number of different silanes.

A 42 amu (SiCH₂) peak appeared at higher laser fluences and ultimately became larger than the 43 amu (MeSi) peak. This peak also likely arises from a two-photon process.

Photolysis of (Me₂Ge)₆. Typical photolysis results for the cyclic polygermane (Me₂Ge)₆ are shown in Figure 3. All significant photolysis-induced peaks are in the mass range shown. The major structure arises from Ge (predominant mass at 74 amu), MeGe (predominant mass at 89 amu), Me₂Ge (predominant mass at 104 amu), and Me₃Ge (predominant mass at 119 amu). The

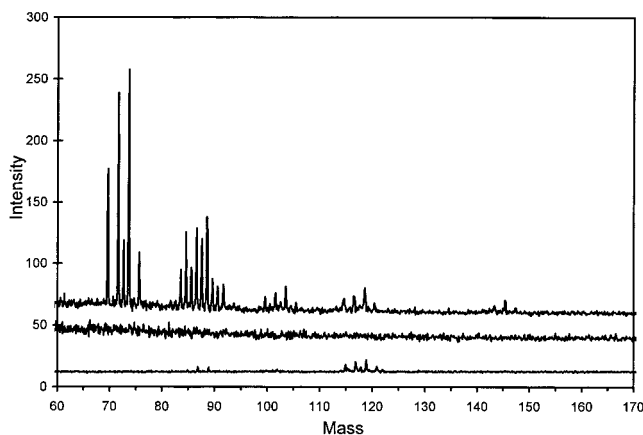


Figure 3. Mass spectrum monitoring the following 193 nm photolysis of $(\text{Me}_2\text{Ge})_6$ (**2**) and subsequent 118 nm photoionization (upper scan). The middle scan is with 193 nm photolysis pulses only and the bottom scan with 118 nm pulses only.

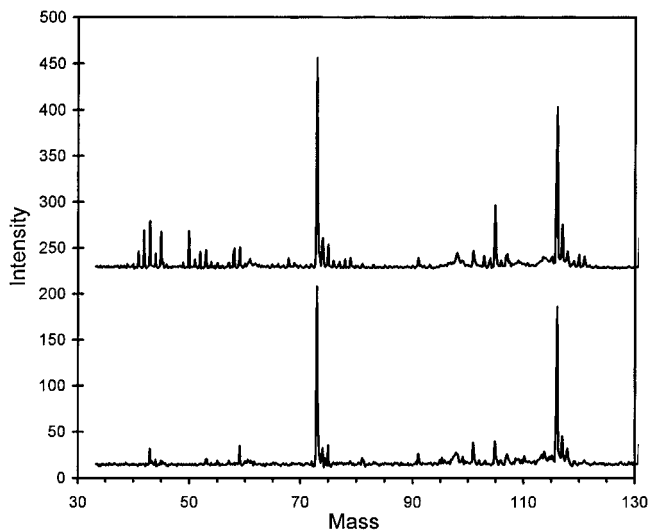


Figure 4. Mass spectrum following 193 nm photolysis of 2-phenylheptamethyltrisilane (compound **1**) and subsequent 118 nm photoionization (upper scan). The lower scan is with 118 nm pulses only.

peaks associated with Me_3Ge are almost entirely due to the photoionization and are not associated with the 193 nm photochemistry. There is more complexity for each of the foregoing species in the germanium analogue compared to silicon because germanium has five isotopes with significant natural abundance. Additional complications, as seen in the MeGe peaks, can arise from the loss of one or more hydrogens. Consistent with the silicon analogue results, and of central interest to us, is the production of a nontrivial amount of Me_2Ge .

While photolysis of $(\text{Me}_2\text{Si})_6$ resulted in significant production of Si_2C , there is no analogous observed production of Ge_2C (expected mass centered at 160 amu) with $(\text{Me}_2\text{Ge})_6$.

Photolysis of 2-Phenylheptamethyltrisilane (1). Representative broad-scale mass spectra (Figure 4) show that the 118 pulses themselves produce many ionic fragments. Significant product peak growth due to the 193 nm photolysis pulses is evident in the 40–60 amu range. The product at 43 amu can likely be associated with MeSi . Other photolysis peaks that can be associ-

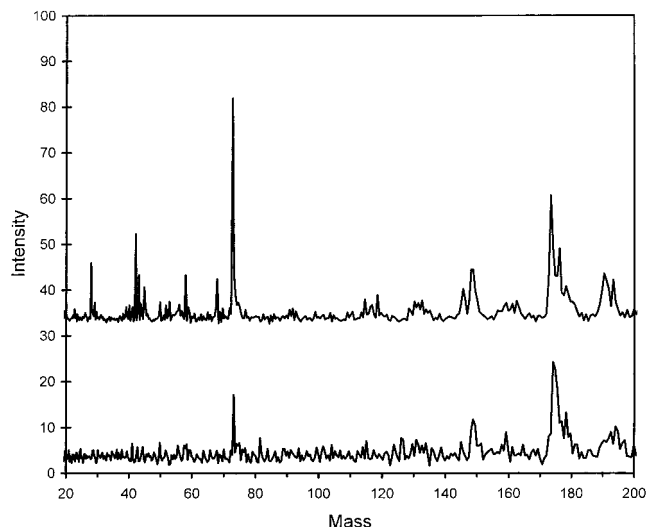


Figure 5. Mass spectrum following 193 nm photolysis of 2-phenyl-2-(trimethylsilyl)hexamethyltrisilane (**2**) and subsequent 118 nm photoionization (upper scan). The lower scan is with 118 nm pulses only.

ated with definite species are at 68 amu (Si_2C) and 105 amu (PhSi).

The product of primary interest is the silylene PhMeSi (120 amu). Sufficiently high laser fluences do lead to production of a small 120 amu product peak. Meaningful power dependence studies on this peak were not possible, but several considerations indicate that the peak arose from higher order processes. It does not appear at lower laser fluences, when only weak product peaks at 43 and 105 amu were evident. It is not certain that the foregoing MeSi and PhSi fragments arose from one-photon photolysis, but some other fragments that appeared at stronger laser fluences such as Si_2C (68 amu) almost certainly arise from multiphoton processes. It was also the case that for mono- and disilanes similar laser fluences produced significant product peaks that also probably arose from higher order photolysis processes (below). In our earlier studies employing 266 nm photolysis/photoionization⁶ no product at 120 amu was detected, even for the strongest laser fluences.

Photolysis of 2-Phenyl-2-(trimethylsilyl)hexamethyltrisilane (2). Typical results in Figure 5 show again a number of product peaks due to absorbance of 118 nm photons. The principal photochemical product peaks are at 28, 43, 58, 68, and 73 amu. Aside from the 73 amu (Me_3Si) peak, which may substantially arise from one-photon 193 nm photolysis, the likely structures of the other products suggest that they probably arose from higher order processes. Much as with compound **1**, a very small photoproduct peak sometimes appeared at 178 amu, probably corresponding to $\text{Ph}(\text{Me}_3\text{Si})\text{Si}$. As was the case with the silylene in compound **1**, we do not attribute its formation to one-photon 193 nm photolysis but would instead argue that it likely arose from a higher order photolysis process. No such product was observed in our earlier beam experiments using 266 nm photolysis/photoionization pulses.¹¹

(11) In ref 6, the parent mass was incorrectly identified as 338 amu instead of 324 amu; similarly, the fragment corresponding to a loss of one Me_3Si unit should have been identified as mass 251 rather than 265.

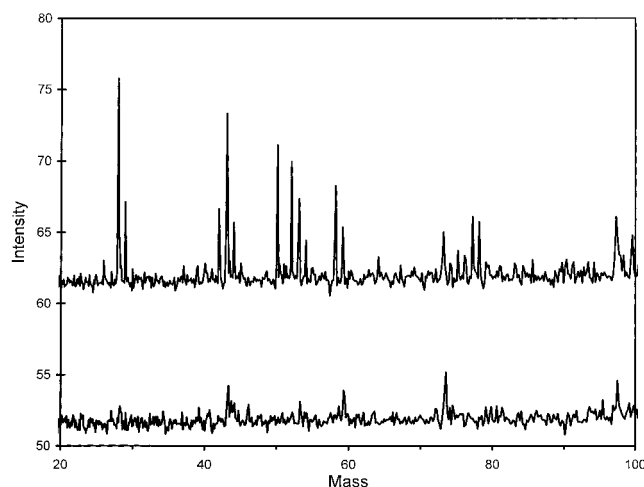


Figure 6. Mass spectrum following 193 nm photolysis of 1,2,2,3-tetramethyl-1,3-diphenyl-1,2,3-trisilacycloheptane (**5**) and subsequent 118 nm photoionization (upper scan). The lower scan is with 118 nm pulses only.

Photolysis of 1,2,2,3-Tetramethyl-1,3-diphenyl-1,2,3-trisilacycloheptane (5**).** Principal photolysis peaks are shown in Figure 6. No significant photolysis product peaks appeared at higher mass. In this instance a significant 58 amu peak appeared, corresponding to Me_2Si . Similar results also were obtained using 222 nm photolysis pulses. Three different independent power dependence plots each showed the photolysis process to be first order for the 58 amu peak.

Photolysis of Vinyltrimethylsilane, Hexamethyldisilane, and Phenyltrimethylsilane. Since the linear polysilanes **1** and **2** produced trimethylsilyl radical as a major photoproduct in the molecular beams, independent trimethylsilyl radical generators were sought in order to interpret their fragmentation pattern. Vinyltrimethylsilane, hexamethyldisilane, and phenyltrimethylsilane were therefore examined as potential sources of trimethylsilyl radical in the gas phase.¹² A trimethylsilyl (73 amu) peak was produced by all these precursors upon 118 nm photoionization alone; however, only vinyltrimethylsilane and hexamethyldisilane resulted in substantial increases in this mass upon 193 nm photolysis irradiation.

The 193 nm photolysis of vinyltrimethylsilane (Figure 7) resulted in an increase in the 73 amu peak as well as a small but clear 58 amu (Me_2Si) product mass peak. Smaller mass peaks were found at 58, 43, 42, and 28 amu.

The 193 nm photolysis of hexamethyldisilane afforded a more substantial peak at 58 amu along with an increase of the 73 amu peaks, as shown in Figure 8. As with the case of vinyltrimethylsilane, mass peaks at 58, 43, 42, and 28 amu were observed. In addition, a prominent peak at 68 amu was observed. Scatter in power dependence measurements did not allow for an unambiguous determination of the photolysis order for 58 amu product formation, but 68 amu product formation was clearly second order.

Photolysis of phenyltrimethylsilane at 193 nm only resulted in a slight increase of the 73 amu peak relative

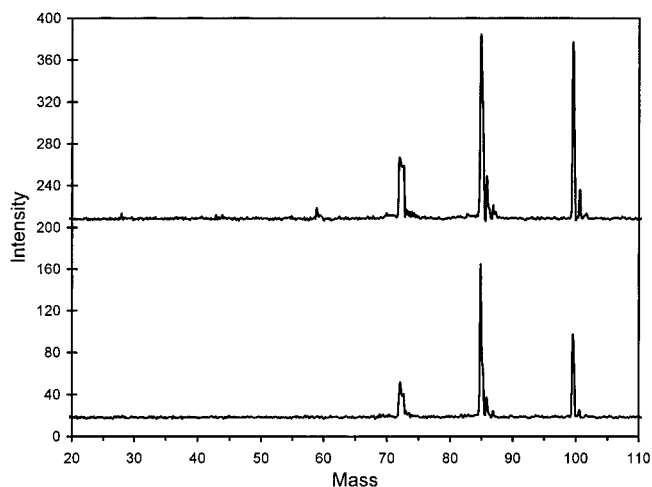


Figure 7. Mass spectrum following 193 nm photolysis of vinyltrimethylsilane and subsequent 118 nm photoionization (upper scan). The lower scan is with 118 nm pulses only.

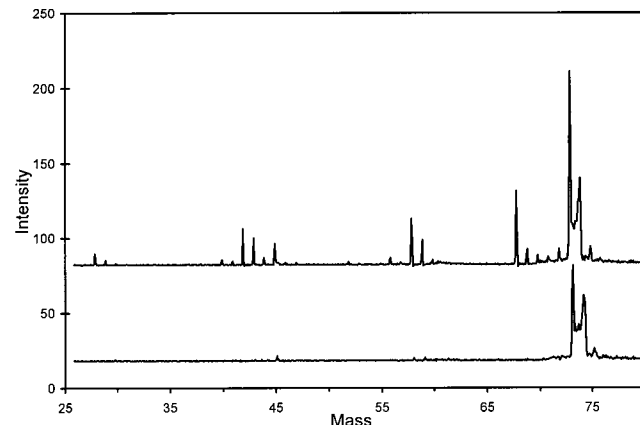


Figure 8. Mass spectrum following 193 nm photolysis of hexamethyldisilane and subsequent 118 nm photoionization (upper scan). The lower scan is with 118 nm pulses only.

to the appearance of new peaks at 77, 53, 52, 50, 46, and 45 amu (Figure 9). A 68 amu peak was also evident following photolysis of phenyltrimethylsilane. Assuming that the product is again Si_2C , it is necessary that an initial photolysis product incorporating one silicon have an encounter with a second species incorporating another silicon. These considerations speak to a strong propensity for formation of Si_2C .

Discussion

The present study extends and improves upon the previous investigation in a number of significant ways. First, two separate lasers were used, one for the photolysis and one for the photoionization. The physical separation of photolysis and photoionization events allow for a more unambiguous determination of photochemical power dependence in many cases. In addition, the 118 nm ionization laser photons are sufficiently high in energy (10.5 eV) to photoionize nearly all possible photofragments.

Photoionization at 118 nm alone, however, occasionally led to significant production of photoionic fragments. This was clearly evident for the photoionization

(12) Hexamethyldisilane has been reported to be a source of trimethylsilyl radical upon 193 nm photolysis in the gas phase. Shimo, N.; Nakashima, N.; Yoshihara, K. *Chem. Phys. Lett.* **1986**, 125, 303.

Scheme 1

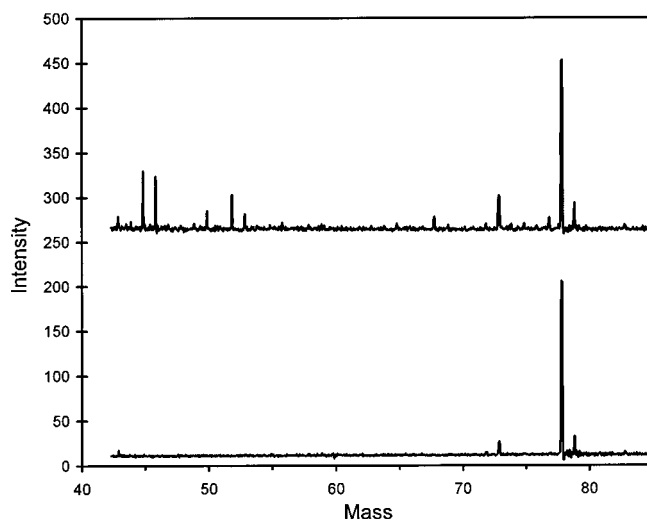
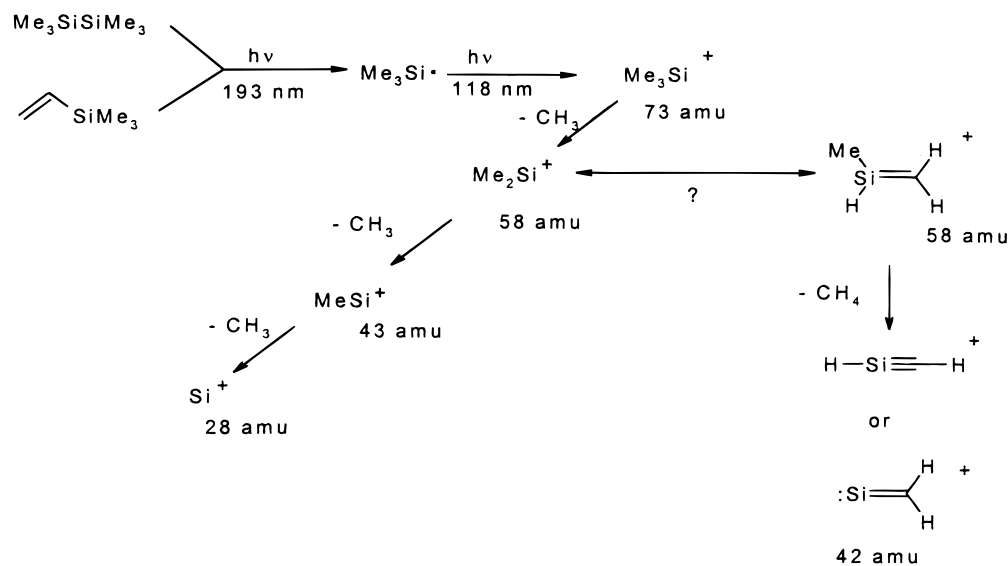


Figure 9. Mass spectrum following 193 nm photolysis of phenyltrimethylsilane and subsequent 118 nm photoionization (upper scan). The lower scan is with 118 nm pulses only.

of all precursors at 118 nm, whereupon fragment ions occurred even in the absence of the photolysis laser. Prior irradiation of the molecular beam by the photolysis laser resulted in the additional appearance of molecular ions of the photoproducts along with their respective daughter ions.

To interpret the photochemical processes involving higher molecular weight precursors, some simple mono- and disilanes were examined. Vinyltrimethylsilane and hexamethyltrisilane were found to be excellent photochemical sources of trimethylsilyl radical ($m/e = 73$ amu). In addition to the 73 amu peak, masses at 58, 43, and 28 amu were also found. These were ascribed to daughter ions of trimethylsilyl radical corresponding to the consecutive loss of methyl groups to give Me_2Si , MeSi , and Si atoms.

A significant 42 amu peak was detected in the photolysis of both vinyltrimethylsilane and hexamethyldisilane. One pathway to this product mass may arise from the dimethylsilylene (Me_2Si) daughter of the trimethylsilyl radical (Scheme 1). Rearrangement of

dimethylsilylene to methylsilene ($\text{Me(H)Si}=\text{CH}_2$) is believed to be nearly isothermal.¹³ Loss of methane by either α -elimination or β -elimination would then give rise to silylidene ($:\text{Si}=\text{CH}_2$) or silyne ($\text{HSi}\equiv\text{CH}$), respectively, with a mass of 42 amu.¹⁴

Phenyltrimethylsilane, in contrast to vinyltrimethylsilane and hexamethyldisilane, was a poor generator of trimethylsilyl radical. Only small amounts of 73 amu ions were produced, as well as the expected fragment ions at 58, 43, and 42 amu. Instead, new masses at 77, 68, 53, 52, 50, 46, and 45 amu were observed. Most of these mass peaks appear to correspond to the fragmentation of either benzene or phenyl radicals. Although a small quantity of atomic Si at 28 amu was observed, no other identifiable silicon-containing fragments were found. This may be due to a much greater photoionization cross section for the aromatic ring relative to the organosilicon fragments. The photolysis of the noncyclic polysilanes yielded masses consistent with the photochemical cleavage of a single silicon-silicon bond. In the case of $\text{PhSi}(\text{SiMe}_3)_3$, a large peak at 73 amu along with masses at 58, 43, 42, and 28 amu clearly showed the presence of trimethylsilyl radical. Additional peaks at 50 and 52 amu arise from phenyl group degradation. The photolysis of $\text{MePhSi}(\text{SiMe}_3)_2$ also gave mass fragments at 73 and 43 amu, indicative of trimethylsilyl radical formation. However, these mass peaks were obscured by fragments from the photoionization of the precursor trisilane and, consequently, the relative intensities of these peaks were difficult to ascertain. Mass fragments from the phenyl group were also conspicuous at 52, 50, and 45 amu. For each trisilane, an extremely weak peak due to the expected silylene was observed. These peaks were only observed under the highest laser

(13) At the best level of theory, Me_2Si is 2 kcal/mol more stable than $\text{Me(H)Si}=\text{CH}_2$ with a barrier height of 41 kcal/mol. (a) Nagase, S.; Kudo, T. *J. Chem. Soc. Chem. Commun.* **1984**, 141. (b) Nagase, T.; Kudo, T.; Ito, K. In *Applied Quantum Chemistry*; Smith, V. H. Jr., Schaefer, H. F., III, Morokuma, K., Eds.; Reidel: Dordrecht, The Netherlands, 1986; pp 249-267.

(14) On the SiCH_2 energy surface, silyne is calculated to be 49.1 kcal/mol less stable than the global minimum silylidene. Isomerization of silyne to silylidene is predicted to have little or no activation barrier: Hoffman, M. R.; Yoshioka, Y.; Schaefer, H. F., III. *J. Am. Chem. Soc.* **1983**, 105, 1084.

fluences used and certainly arose from multiphoton processes.

Photolysis of the cyclic precursor $(\text{Me}_2\text{Si})_6$, in stark contrast to the linear and branched polysilanes, *does* efficiently produce the silylene, Me_2Si . The appearance of the Me_2Si peak (58 amu) is first order with respect to photolysis laser intensity, indicating that it is the result of a one-photon event. This is the first direct observation of Me_2Si in a molecular beam. In our preliminary study,⁶ Me_2Si was inferred indirectly from the observation of the $(\text{Me}_2\text{Si})_5$ coproduct. Additional masses at 43 and 28 amu are likely fragments from the photoionization of Me_2Si , formed by consecutive losses of methyl groups. Power dependence measurements on the intensity of the $(\text{Me}_2\text{Si})_5$ mass peak showed saturation and eventual loss of intensity at very high laser powers. This is probably due to additional photochemistry of $(\text{Me}_2\text{Si})_5$, consistent with the known photoreactivity of this compound in solution.¹⁵

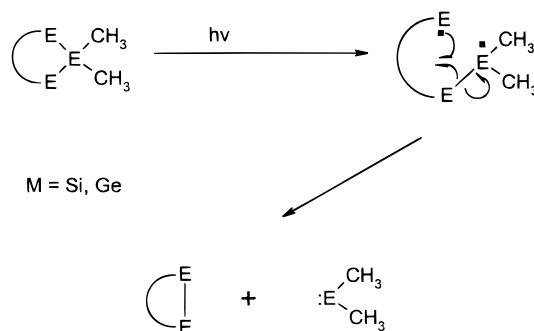
The photolysis of the cyclic germanium compound $(\text{Me}_2\text{Ge})_6$ was completely analogous to that of $(\text{Me}_2\text{Si})_6$. Dimethylgermylene, Me_2Ge , was very cleanly produced during the photolysis, giving the expected isotope cluster centered at 104 amu. Isotope clusters centered at 89 and 74 amu correspond to fragmentation involving loss of methyl groups.

The dramatic difference in photochemistry in going from the cyclic compounds $(\text{Me}_2\text{Si})_6$ and $(\text{Me}_2\text{Ge})_6$ to the radical producing linear and branched polysilanes may rest in differences in electronic properties and/or molecular topology. For instance, the photoreactive excited state of a cyclohexasilane may be so significantly different from that of a linear trisilane that an intrinsically different photochemical outcome may result. On the other hand, differences in photochemistry may be simply attributed to whether the molecule is linear or whether it is cyclic. In an attempt to distinguish these possibilities, we examined the photochemistry of the 1,2,3-trisilacycloheptane **5** in the molecular beam.

In solution, 1,2,3-trisilacycloheptanes photochemically extrude the central silicon atom as a silylene to give 1,2-disilacyclohexanes.¹⁶ For the specific case of **5**, this photoextrusion occurs with retention of stereochemistry for both silicon atoms in the 1,2-disilacyclohexane product.⁸ For our purposes, these compounds are essentially trisilanes with the terminal silicon atoms tethered by an electronically insulating tetramethylene bridge. These precursors therefore should be virtually identical with the linear trisilanes in electronic structure but are constrained to a cyclic structure.

The trisilacycloheptane **5** is an efficient photochemical generator of a silylene. This is apparent from the intense peaks due to dimethylsilylene (58 amu) and its daughters at 43, 42, and 28 amu. Present with lesser intensity were peaks at 50, 52, and 78 amu, indicative of phenyl group fragmentation. The dramatic difference in photochemical outcome between this cyclic trisilane and the two noncyclic ones strongly suggest that silylene (and germylene) formation lies not in the nature of the excited state but is dependent on the geometric constraints of a cyclic system.

Scheme 2



Our results suggest a common mechanism for polysilane photolysis in the gas phase in which the primary photochemical event is the homolytic cleavage of a single silicon-silicon bond. For noncyclic polysilanes, the resulting silyl radicals recoil from each other and become the ultimate detectable products. Homolytic Si-Si cleavage in cyclic systems, on the other hand, yield α,ω -diradicals which are capable of subsequent intramolecular reactions. Silylene formation subsequently becomes possible by an $\text{S}_{\text{H}2}$ mechanism by which a Si-Si bond is attacked by the distal silyl radical (Scheme 2). $\text{S}_{\text{H}2}$ displacements of Si-Si bonds are well-precedented reactions.¹⁷

The reaction rate for the second thermal step which generates the silylene must be very high. In solution, the trisilacycloheptane **5** is known to produce dimethylsilylene with the retention of stereochemistry at both silicon atoms. Any intermediate diradical therefore must extrude silylene at a rate greater than that of a silicon-carbon bond rotation. The elusiveness of diradicals to spectroscopic detection in the solution photolysis of cyclic silylene precursors may be a testament to their high reactivity and very short lifetimes.

The proposed mechanism may be cautiously extended to the condensed phase, in which the silicon-containing precursors **1-3** and **5** are all observed to generate silylenes. Although linear and branched polysilanes give only silyl radicals under molecular beam conditions, they are highly efficient silylene precursors in solution and in cold matrices.^{4,5} This apparent discrepancy is still reconcilable by a common primary photochemical step. In the condensed phases, the radical pair generated is initially bound in either a solvent or matrix cage where further reaction chemistry may take place. The $\text{S}_{\text{H}2}$ displacement of the Si-Si bond of one radical by the other may effectively generate the silylene and disilane products in a mechanistic step similar to that proposed for the cyclic precursors in the gas phase. Again in such a case, the second bimolecular step for the production of silylene must be very fast and efficient in order to be competitive with radical separation from the cage.

Although it is tempting to accept such a $\text{S}_{\text{H}2}$ mechanism as a general process for the production of silylenes in the condensed phase, theoretical studies and experimental results strongly suggest a concerted extrusion under these conditions. Particularly convincing is the photochemical extrusion of dimethylsilylene from **5** with the retention of stereochemistry¹⁶ and the

(15) In solution, $(\text{Me}_2\text{Si})_5$ photochemically decomposes to $(\text{Me}_2\text{Si})_4$ with the extrusion of Me_2Si : Ishikawa, M.; Kumada, M. *J. Organomet. Chem.* **1972**, 42, 325.

(16) Sakurai, H.; Kobayashi, Y.; Nakadaira, Y. *J. Am. Chem. Soc.* **1971**, 93, 5292.

(17) $\text{S}_{\text{H}2}$ reactions are known to occur at Si-Si bonds: (a) Hosomi, A.; Sakurai, H. *J. Am. Chem. Soc.* **1972**, 94, 1384. (b) Nakadaira, Y.; Sakurai, H. *J. Organomet. Chem.* **1973**, 47, 61.

photochemical ring contraction of a "racked" dodecamethylhexasilane with the concomitant extrusion of dimethylsilylene.¹⁸ A recent detailed study by Kira on the photochemistry of the linear trisilane $\text{Ph}_2\text{Si}(\text{SiMe}_3)_2$ also strongly suggests that the extrusion of diphenylsilylene is concerted in solution.¹⁹

In most cases, it is believed that the concerted silylene extrusion arises from excited singlet states of the polysilane.²⁰ While these reactive singlet states may predominate in solution, other radical producing states may be much more important for isolated molecules in the gas phase. It has been proposed that both triplet²¹ and Rydberg states^{20a,22} may also be important in the photochemistry of polysilanes. The observation of radical products in the gas-phase experiments may possibly be the result of these states. Further experiments are still needed, both in the gas phase and in solution, to understand the relative importance of all of the various reactive excited states of polysilanes.

Finally, in the photolysis of many organosilicon precursors, a prominent mass at 68 amu is found. This ubiquitous peak is ascribed to Si_2C on the basis of isotope cluster intensities. This bent triatomic molecule has been characterized experimentally²³ and theoretically.²⁴ Whereas Si_2C has been typically produced in the past by laser vaporization of silicon carbide²⁵ or vaporization of solid silicon and carbon,²⁶ we have for the first time produced Si_2C via photolysis of gas-phase precursors. Where power dependences can be determined, the appearance of Si_2C is second order in photolysis laser intensity. It is noteworthy that Si_2C is present even when the gas-phase precursor has one silicon atom, possibly implying its formation under plasma conditions

where bimolecular chemistry may occur. The general appearance of this ion may be due to a remarkable stability relative to other small silicon molecules, a fact that possibly has astrophysical implications.

Conclusions

Photochemical silylene precursors in the condensed phase do not always photochemically generate silylenes in the gas phase under molecular beam conditions. Of the condensed-phase organosilylene precursors examined, only the cyclic polysilanes **3** and **5** give organosilylenes in significant quantities. An analogous processes is also seen for the cyclic polygermane **4** to give a germylene. The linear and branched polysilanes **1** and **2**, in contrast, give photochemical products derived from the homolytic cleavage of a single Si–Si bond. The difference in photochemical outcome between these two sets of polysilanes appears to derive from molecular topology (cyclic vs noncyclic) rather than inherent electronic effects. This is most clearly demonstrated by the strikingly different photochemical outcomes of the cyclic trisilane precursor **5**, which produces a silylene, and the electronically similar linear trisilane **1**, which produces only silyl radicals.

A unifying mechanism which would account for the observed photochemical behavior in the gas phase involves the initial homolytic cleavage of a Si–Si bond for all silicon precursors. For the noncyclic precursors, the resulting silicon radicals cannot undergo further bimolecular reactions in the gas phase. However, the α,ω -diradicals produced from cyclic precursors can subsequently react to give silylenes via an intramolecular scission. This mechanism may also be operable in the condensed phase as well, but probably only as a minor pathway. The observation of extensive homolytic scission in the gas phase is likely due to excited states not readily accessible in solution. Experiments to further elucidate photochemical processes both in a molecular beam and in the condensed phase are currently underway.

Acknowledgment. We gratefully acknowledge support from the Department of Chemistry, the DoE/Epscor program, and the Center for Photoinduced Processes, funded by the National Science Foundation and the Louisiana Board of Regents.

OM990880U

(18) Mazieres, S.; Raymond, M. K.; Raabe, G.; Prodi, A.; Michl, J. *J. Am. Chem. Soc.* **1997**, *119*, 6682.

(19) Miyazawa, T.; Koshihara, S.; Liu, C.; Sakurai, H.; Kira, M. *J. Am. Chem. Soc.* **1999**, *121*, 3651.

(20) (a) Halevi, E. A.; Winkelhofer, G.; Meisl, M.; Janoschek, R. *J. Organomet. Chem.* **1985**, *294*, 151. (b) Balaji, V.; Michl, J. *Polyhedron* **1991**, *10*, 1265.

(21) Venturini, A.; Vreven, T.; Bernardi, F.; Olivucci, M.; Robb, M. A. *Organometallics* **1995**, *14*, 4953.

(22) Bock, H.; Wittel, K.; Veith, M.; Wiberg, N. *J. Am. Chem. Soc.* **1976**, *98*, 109.

(23) Presilla-Marquez, J. D.; Graham, N. R. M. *J. Chem. Phys.* **1991**, *95*, 5612.

(24) Bolton, E. E.; DeLieuw, B. J.; Fowler, J. E.; Grev, R. S.; Schaefer, H. J. III. *J. Chem. Phys.* **1992**, *97*, 5586 and references therein.

(25) Weltner, W., Jr.; McLeod, D., Jr. *J. Chem. Phys.* **1964**, *41*, 235.

(26) Presilla-Marquez, J. D.; Graham, W. R. M. *J. Chem. Phys.* **1991**, *95*, 5612.